Near-source and remote observations of kilometric continuum radiation from multi-spacecraft observations

J. D. Menietti, R. R. Anderson, J. S. Pickett, and D. A. Gurnett

The University of Iowa, Department of Physics and Astronomy, Iowa City, IA

January 2003

Submitted to:

Journal of Geophysical Research

Abstract. Kilometric continuum (KC) radiation was first identified from Geotail plasma wave observations. Past authors have shown that this emission has a frequency range that overlaps that of the auroral kilometric radiation (AKR), but is characterized by a fine structure of narrow-bandwidth, linear features that have nearly constant or drifting frequency. This fine structure is distinct from that of AKR. KC also apparently has a distinct source region probably associated with the low-latitude inner magnetosphere, consistent with direction finding and ray tracing results. We present new observations of KC obtained by the Polar plasma wave instrument in the near-source region. These observations show intense electrostatic and less intense electromagnetic emissions near the magnetic equator at the plasmapause. Simultaneously, Geotail, located at 20 to 30 R_E in radial distance, observes KC in the same frequency range. These data suggest a possible mode-conversion source mechanism near a region of high density gradient. High resolution data obtained from wideband receivers on board both Polar and Cluster show closely-spaced bands of emission near the magnetic equator that may be due to many nearby independent sources of EM emission that may be associated with density fluctuations or cavities in the plasmasphere.

1. Introduction

Brown [1973] and *Gurnett and Shaw* [1973] first reported terrestrial nonthermal continuum emission in a broad frequency range extending from ~5 kHz to < 100 kHz. The term continuum implied a diffuse, rather continuous spectrum. *Gurnett and Shaw* [1973] and *Gurnett* [1975] proposed a source near the dawnside plasmapause, with a source mechanism associated with intense upper hybrid waves. *Kurth et al.* [1981] and *Kurth* [1982] described the details of the narrow-banded escaping component of continuum emission providing clear evidence of its narrow-bandedness associated with intense upper hybrid (UH) resonance emissions. These emissions are also believed to have a low-latitude source in the outer plasmasphere and in the magnetopause [*Morgan and Gurnett*, 1991]. The source mechanism of this continuum emission has been proposed to be a mode conversion process occurring near the dayside magnetopause and/or the nightside plasmapause near the equator. Both linear [e.g., *Jones*, 1976, 1988; *Budden*, 1980] and non-linear [cf. *Melrose*, 1981; *Fung and Papadopoulos*, 1987; *Ronnmark*, 1983] classes of mode conversion have been suggested as summarized in *Kurth et al.* [1992].

Hashimoto et al. [1999] have described kilometric continuum (KC) as emission that lies in the same frequency range as auroral kilometric radiation (AKR) [cf. *Gurnett*, 1974], but with a different spectral morphology and a unique source region, the low-latitude inner plasmasphere. KC was observed by Geotail (in an equatorial orbit) to consist of slowly drifting narrowband signals in the frequency range 100 kHz < f < 800 kHz. Direction-finding using spin modulation of the emission at 400 kHz indicated the source of the emission is consistent with the low-magnetic-latitude inner plasmasphere. The emission thus has much in common with non-terrestrial continuum emission observed at lower frequencies (typically < 100 kHz). More recently, *Green et al.* [2002a,b] have shown an association of the kilometric continuum with

plasmaspheric notches (bite-outs) of density and suggested that these large-structure cavities may be a source region of the KC.

In this paper we show joint observations of Polar and Geotail plasma wave data. Geotail observes KC at distances > 10 R_E while Polar passes through the magnetic equator near the plasmapause and the proposed source region of KC. In addition we include some unique, high-resolution data obtained by the wideband receivers on board both Polar and the Cluster spacecraft that provide new and interesting information regarding the source region and possible density structure of the outer low-latitude plasmasphere.

2. Instrumentation

2.1. Polar

The Polar satellite was launched in late February 1996 into a polar orbit with apogee of about 9 R_E and a perigee of about 2.2 R_E. Polar is the first satellite to have 3 orthogonal electric antennas (E_u, E_v, and E_z), 3 triaxial magnetic search coils, and a magnetic loop antenna, as well as an advanced plasma wave instrument [*Gurnett et al.*, 1995]. This combination can potentially provide the polarization and direction of arrival of a signal without any prior assumptions.

The Plasma Wave Instrument on the Polar spacecraft is designed to provide measurements of plasma waves in the Earth's polar regions over the frequency range from 0.1 Hz to 800 kHz. Five receiver systems are used to process the data: a wideband receiver, a high-frequency waveform receiver (HFWR), a low-frequency waveform receiver, two multichannel analyzers, and a pair of sweep frequency receivers (SFR). For the high frequency emissions of interest here, the SFR is of special interest. The SFR has a frequency range from 24 Hz to 800 kHz in 5 frequency bands. The frequency resolution is about 3% at the higher frequencies. In

the log mode a full frequency spectrum can be obtained every 33 seconds. From 12.5 to 800 kHz, of interest in this study of KC, a full frequency spectrum can be obtained every 2.4 seconds.

The wideband receiver (WBR) provides high-resolution waveform data, and is programmable allowing the selection of 11, 22, or 90 kHz bandwidths with a lower band edge (base frequency) at 0, 125, 250, and 500 kHz. In the 90 kHz bandwidth mode the sampling rate is 249 kHz.

2.2. Geotail

Geotail was launched into a low-inclination orbit, and since February 1995 this orbit has been elliptical with a perigee of about 10 R_E and an apogee of about 30 R_E.

The Sweep-Frequency Analyzer (SFA) on Geotail is comprised of eight receivers that measure the electric field over the range of 24 Hz $< f <$ 800 kHz, and the magnetic field over the range 24 Hz $< f <$ 12.5 kHz. In the KC frequency range there are two receivers. One operates in the range 12.5 kHz to 100 kHz in 680 Hz steps, and the other operates over the range 100 to 800 kHz in 5.4 kHz steps. The instrument uses two spin-plane electric dipole antennas with a tip-to-tip length of 100m [cf. *Matsumoto et al.*, 1994].

2.3. Cluster

The Cluster II mission consists of four identical satellites in a high-inclination orbit with a nominal apogee of 12 R_E and perigee of 2 R_E. The mission objectives include studies of the magnetopause and magnetotail reconnection sites and magnetospheric phenomena.

The wideband plasma wave investigation on Cluster is part of the Wave Experiment Consortium (WEC), which consists of five instruments designed specifically to study

magnetospheric wave phenomena [*Pedersen et al.*, 1997]. The Cluster mission and wideband instrument have been described in previous publications [cf. *Gurnett et al.*, 2001]. The objective of the wideband plasma investigation is to provide very high-time resolution measurements in order to resolve spatial and temporal structure in the plasma waves and magnetosphere. The investigation consists of four identical instruments (one on each spacecraft) called the Wideband (WBD) plasma instruments. These instruments measure electric or magnetic field waveforms in one of three possible bandwidths: 25 Hz to 9.5 Hz, 50 Hz to 19 kHz, or 1 Hz to 75 kHz. The base frequency (frequency offset) can be programmed to be either 125 kHz, 250 kHz, or 500 kHz. The bit rate in the real time mode of operation is 220 kbits/s.

3. Observations

We have examined a large portion of the Polar SFR data and the Geotail SFA data for examples of possible encounters with KC emissions. The orbits of the two satellites during 1996-1997 made these two instruments particularly well-suited for a joint study. Polar was placed in a 90-degree inclination orbit with an apogee of about 9 R_E and a perigee of about 1.8 R_E. The orbital period is about 18 hours. Polar passed through the nightside equatorial region near the plasmapause (4-5 R_E), and at somewhat lower distances (2.5 - 3.5 R_E) on the dayside during the period of analysis in this study. During this period the apogee was over the northern polar cap and perigee over the southern polar region. The Geotail satellite orbit during 1996 to 1997 was in an equatorial orbit with a nightside apogee of about 30 R_E and a dayside perigee of about 10 R_E, and the orbital period was about 1.5 days. The purpose of the present study was to investigate observations of kilometric continuum emission (KC) observed by both satellites,

particularly simultaneous observations. The orbit of Polar brought it near the proposed source region of KC, near the equatorial plasmapause [*Hashimoto et al.*, 1999; *Green et al.*, 2002a].

We have chosen a number of interesting examples to display. These cases represent times when the PWI detected electromagnetic (EM) emission near the upper hybrid frequency, f_{UH}, generally when the spacecraft was near the magnetic equator. This is not a comprehensive study of all of the equator passes, but does represent a sizeable sampling of the data.

We start with data from May 20, 1996, when Polar at lower-altitude and Geotail at higher altitude are simultaneously monitoring the same magnetic local time (MLT). In Figure 1 we display a frequency-time spectrogram of the Geotail plasma wave instrument sweep-frequency analyzer with relative power gray-coded. This spectrogram covers a six-hour period when the spacecraft was on the nightside at a distance ranging from 15.75 R_E to 12.3 R_E, and ranging in magnetic latitude from 8.4° through the magnetic equator to -6.1°. The near constant-frequency structures extending in frequency from 100 kHz to over 600 kHz are kilometric continuum emission and are distinguished morphologically from the more broad-banded structures comprising the auroral kilometric radiation (AKR). We will concentrate on a 25-minute time period from 03:40 to 04:05 that is displayed in the Polar PWI sweep-frequency receiver (SFR) data in Figure 2. Here the MLT is near 22 hours and the spacecraft varies in radial distance from 4.11 to 3.58 R_E. The magnetic latitude, λ_m, varies in the polar orbit from 15° to < 4.7°. The top panel displays the electric field while the bottom panel shows the magnetic field data in a frequency range from 100 kHz to 250 kHz. These spectrograms show a banded electromagnetic emission with separation of the bands consistent with harmonics of the local cyclotron frequency, f_{ce}, which varies from about 12.5 to 19 KHz over this time range. This emission could be KC near its source in the frequency range of 150 to 200 kHz.

In Figure 3 we show a much higher resolution spectrogram that covers only two minutes of time. Here a spin modulation of the electric and magnetic field data is discernable. The spin period of the Polar satellite is about 6 seconds while the nulls in Figure 3 are about 10 seconds apart. This is due to an aliasing of the spin period with the instrument frequency cycling period of about 2.4 seconds. We have determined the angle between the PWI E_u antenna and the local magnetic field for this time period. The peaks in the electric field intensity occur when the antenna is nearly perpendicular to the ambient magnetic field, **B**, while the oscillating magnetic field intensity shown in the lower panel shows intensity maximum that are almost aligned with **B**. These observations are consistent with electrostatic upper hybrid emission and electromagnetic ordinary mode emission. This example is similar to numerous other examples of well-organized spin modulation data.

In Figure 4 we show a spectrogram of Polar SFR data for a one-hour period on day February 11, 1997. During this time period the spacecraft is located in the afternoon sector with MLT ranging from 15.0 hours to 16.1 hours. The radial distance varies from 2.11 R_E to 3.4 R_E. Significantly the magnetic latitude varies from high southern latitudes, -38.2° through the magnetic equator to ~14.4°. The electric field data show a band of upper hybrid emission centered near 200 kHz with two regions of more enhanced emission near 15:20 and $\lambda_m \sim -23.5°$ and again near the magnetic equator at about 15:43 spacecraft event time (SCET). During both of these times the emission becomes electromagnetic as seen in the bottom panel. During this same time period Geotail observed KC and was located in the MLT range of 15.9 hours $\lesssim$ MLT $\lesssim$ 16.2 hours, 14.3 $R_E < R < 14.9\ R_E$, and $7.5° < \lambda_m < 10.4°$. If the EM emission observed by Polar is KC, then it is observed at a magnetic latitude that is significantly higher than 10°, which

Hashimoto et al. [1999] reported as the nominal maximum magnetic latitude of KC emission observed by Geotail.

In Figure 5 we show Geotail observations for May 23, 1996. Polar observations for the period from 02:10 to 02:32 are compared in Figure 6. We note that Geotail at this time is located at R ~30.25 R_E, MLT ~14.55 hours, and λ_m ~14.1 degrees, while Polar was in the range 3.1 R_E < R < 3.7 R_E, -4.9° < λ_m < 7.75°, and 21.9 hours < MLT < 22 hours. Thus, Polar is about 8 hours away in MLT. It would be unlikely that a plasmaspheric density notch would extend in longitude for this range. In Figure 6 we observe several bands of UH emission in the electric field data and a few bands of EM emission in the magnetic field data of the lower panel. The bands of emission are separated by ~20 kHz, consistent with the local value of f_{ce} which, during this time period, lies in the range 16 kHz < f_{ce} < 24 kHz. Spin modulation is clearly seen in the Polar data and analyses of the antenna orientations relative to the local ambient magnetic field give results consistent with those for the data of May 20, 1996, shown in Figure 3. The electric field data are consistent with UH emission while the magnetic data are out of phase by 90° in spacecraft rotation and thus indicate possible ordinary mode emission.

In Figure 7 we show an example of Polar SFR data for May 15, 1996. The spacecraft is located in the range 3.8 < R < 5.3 R_E, - 7.0° < λ_m < 13.2°, and MLT ~22.3 hours. The interesting aspect of this data is the clear oscillation of the UH signature in both the electric and magnetic field indicating a probable density fluctuation, perhaps due to the spacecraft crossing a density duct or encountering a density cavity. The density cavity appears to extend several degrees in magnetic latitude. At this same time period, Geotail detected clear signatures of KC emission over the frequency range 100 kHz < f < 800 kHz, but the spacecraft was located on the dayside near 9 hours MLT. This example of oscillations of the UH emission in the Polar UH wave

emission is certainly not unique. Numerous other examples with corresponding EM emission have been discovered in the Polar PWI data.

The high resolution wideband data of the PWI is not often available during magnetic equator crossings. However, on April 10, 1996, we were fortunate to have a time interval in which the instrument was operating in the correct frequency range. In Figure 8 we show the spectrogram of the data from the SFR. This data looks typical of many of the other crossings of the magnetic equator, this time located at MLT ~0.35 and R ~4.5 R_E. There is some rather intense electric field emission and faint, but distinct magnetic oscillations observed in the interval from about 15:27 to 15:32. In Figure 9 we show the wideband receiver data for a 48-second time interval starting at 15:30.046. This data covers a frequency range from 125 kHz to about 215 kHz, which includes the EM emission seen in Figure 8. Of particular significance in Figure 9 are the many relatively intense near-constant frequency emission bands observed. In the frequency range 150 kHz $< f <$ 170 kHz the separation of the bands is in the range of 2 to 3 kHz, whereas the spacing is even less for $f >$ 170 kHz. There is also a spin-modulation of the data showing nulls at ~3 second intervals. This modulation is consistent with electrostatic UH emission for the most intense bands in the interval 150 kHz $< f <$ 170 kHz. We note, however, that the emission at higher frequencies, $f \geq$ 170 kHz, shows emission maxima and nulls that are ~90° out of phase relative to the lower frequency emission. This indicates emission consistent with the ordinary mode. The local cyclotron frequency at this time is about 9 kHz, and is much larger than the approximate separation of the bands seen in Figure 9. Therefore these bands most likely do not represent harmonics of local f_{ce}.

The Cluster spacecraft orbit intercepts the magnetic equator near the plasmapause during 2002, and we were fortunate to have the plasma wave wideband instrument in a fortuitous

operating mode on June 19, 2002. In Figure 10 we display a spectrogram of the wideband instrument for the SC2 spacecraft. The spectrogram covers a frequency range from 250 kHz to 260 kHz over a 30-second time interval. The spacecraft is located just above the magnetic equator at λ_m ~3.2°, R = 4.36 R_E and MLT ~17 hours. Seen in the figure are very many closely-spaced emission bands that increase slightly in frequency over the 30 second period of the plot. Spin modulation lanes are also seen at about 2 second intervals. The similarity between this plot and Figure 9 is striking. The difference is in the frequency resolution. While operating in the 10 kHz bandwidth mode, Cluster has a higher frequency resolution than the Polar wideband instrument, and is capable of detecting emission differences of ~100Hz in this frequency range. In Figure 10 the band separations discernable are only a few hundred Hz and perhaps smaller. The cyclotron frequency for this time period is approximately 10 kHz, so that the bands of Figure 10 are much too close to represent harmonics of f_{ce}.

4. Summary and Conclusions

We have presented plasma wave data from three satellites that suggest kilometric continuum emission has a source in the low-latitude plasmasphere as has been argued by *Hashimoto et al.* [1999]. The Polar spacecraft orbit allowed direct observation of magnetic equator crossings in the range of distances from ~2.5 R_E (dayside) to ~4.5 R_E (nightside) during 1996 and 1997. On many passes Polar observed upper hybrid emission near the higher density regions in the vicinity of the magnetic equator as has been reported often in the past [cf. *Kurth*, 1982]. Often this emission was accompanied by EM emission detected by the magnetic receiver of the Polar PWI. On numerous passes, this emission was observed simultaneously with Geotail observations of kilometric continuum, when Geotail and Polar were near the same MLT and both

close to the magnetic equator. Other similar EM observations were made when Polar and Geotail were well-separated in MLT. The Polar SFR observations are typically banded with separations in frequency consistent with the local cyclotron frequency. Spin-modulation observed by the Polar observations indicate the electric field emission is consistent with UH waves, and the magnetic oscillations are consistent with ordinary mode emission.

Green et al. [2002a,b] have reported that kilometric continuum appears to have a source within the plasmasphere density notch or bite-out region. These regions have been detected in images obtained from the extreme ultraviolet (EUV) imager on board the IMAGE satellite which was launched in 2001. As reported by *Green et al.* [2002a] these notch regions are of large scale with extents of perhaps 10° to 15° with density depletions of perhaps 90% of the local nominal value. Our Polar observations cannot confirm that the EM emission is within a density notch, but several observations of oscillating frequency of UH emission indicate fluctuations in local density values of a somewhat smaller size scale, such as those seen in Figure 7. The simultaneous observations of Polar and Geotail, when the two spacecraft are well-separated, could only be associated with a plasmaspheric density notch if there was more than one notch in the plasmasphere at the time. It is also interesting to note that Polar PWI observed EM emission within the plasmasphere at relatively high latitude, well above the ±10° limits set for KC by *Hashimoto et al.* [1999] (cf. February 11th observations, Figure 2).

If the EM emissions observed by Polar are KC that is identified in the Geotail spectrograms, then our results indicate that KC emission is not necessarily confined to plasmaspheric notch regions. This is true because Polar observed this emission typically as it neared the magnetic equator, independent of the location of Geotail. Unless the plasmaspheric notches are much more common than observations to date imply, then Polar observations imply

that the presence of a density notch is not necessary for the generation KC. However, the notch may focus the KC emission via refraction so that it is more easily detected by a remote satellite [cf. *Green et al.*, 2001a].

The wideband observations of Polar and Cluster provide new and interesting information. Multiple closely-spaced (in frequency) bands observed by both spacecraft near the magnetic equator and within the plasmasphere indicate that the emission is not just due to harmonics of f_{ce}. One explanation for such emission is that it is due to multiple UH sources or ordinary mode emission from source regions located at different radial distances (hence frequency). A radial separation of < 1000 km could explain differences of f_{ce} of only a few hundred Hz. If the lines observed in Figures 9 and 10 are due to UH resonances, then density fluctuations would also be important because $f_{UH} = \sqrt{(f_p^2 + f_{ce}^2)}$, where f_p is the plasma frequency. It is conceivable that density fluctuations in the form of cavities or ducts may be present. Density cavities have recently been reported by Decreau [private communication, 2002] by the Cluster WAVES experiment [e.g. *Moullard et al.*, 2002].

The source mechanism of KC emission is probably the same as that of the terrestrial and planetary non-thermal continuum which has been generally described by the linear conversion theory of *Jones* [1988] or by the non-linear conversion mechanisms described by *Melrose* [1981], *Barbosa* [1982], or *Ronnmark* [1983, 1989, 1992]. All of these mechanisms involve upper hybrid waves. In the linear mechanism UH waves refract (in a steep density gradient) to z-mode waves at a wave normal angle near 90°. Z-mode waves can mode convert to O-mode waves [cf. *Horne*, 1989, 1990]. The non-linear mechanisms are described by the authors as more efficient than the linear conversion mechanism. For these processes UH waves coalesce with some lower frequency wave. The polarization and wave modes obtained by Polar are consistent

with these theories, but we cannot easily distinguish between them. It is hoped that future Cluster observations may help resolve some of these outstanding questions regarding the source of KC.

Acknowledgments. The authors thank J. Hospodarsky for text editing. The research at Iowa was supported by NASA grant NAG5-11942 and NAG5-9561.

References

Barbosa, D. D., Low-level VLF and LF radio emissions observed at Earth and Jupiter, *Rev. Geophys.*, *20*, 316-334, 1982.

Brown, L. W., The galactic radio spectrum between 130 kHz and 2600 kHz, *Astrophys. J.*, *180*, 359-370, 1973.

Budden, K. G., The theory of radio windows in the ionosphere and magnetosphere, *J. Atmos. Terr. Phys.*, *42(3)*, 287-298, 1980.

Fung, S. F., and K. Papadopoulos, The emission of narrow-band Jovian kilometric radiation, *J. Geophys. Res.*, *92*, 8579-8593, 1987.

Green, J. L., B. R. Sandel, S. F. Fung, D. L. Gallagher, and B. W. Reinisch, On the origin of kilometric continuum, *J. Geophys. Res.*, *107(A7)*, 1105, doi: 10.1029/2001JA000193, 2002a.

Green, J. L., S. Boardsen, S. F. Fung, H. Matsumoto, K. Hashimoto, R. R. Anderson, B. R. Sandel, and B. W. Reinisch, Association of kilometric continuum radiation with plasmaspheric structures, *J. Geophys. Res.*, in press, 2002b.

Gurnett, D. A., The Earth as a radio source: Terrestrial kilometric radiation, *J. Geophys. Res.*, *79*, 4227-4238, 1974.

Gurnett, D. A., The earth as a radio source: The nonthermal continuum, *J. Geophys. Res.*, *80*, 2751-2763, 1975.

Gurnett, D. A., and R. R. Shaw, Electromagnetic radiation trapped in the magnetosphere above the plasma frequency, *J. Geophys. Res.*, *78*, 8136-8149, 1973.

D. A. Gurnett, A. M. Persoon, R. F. Randall, D. L. Odem, S. L. Remington, T. F. Averkamp, M. M. Debower, G. B. Hospodarsky, R. L. Huff, D. L. Kirchner, M. A. Mitchell, B. T. Pham, J. R. Phillips, W. J. Schintler, P. Sheyko, and D. R. Tomash, The Polar Plasma Wave Instrument, *Space Sci. Rev.*, *71*, 597-622, 1995.

Gurnett, D. A., R. L. Huff, J. S. Pickett, A. M. Persoon, R. L. Mutel, I. W. Christopher, C. A. Kletzing, U. S. Inan, W. M. Martin, J. Bougeret, H. St. C. Alleyne, and K. H. Yearby, First Results from the Cluster Wideband Plasma Wave Investigation, *Ann. Geophys.*, *19*, 1259-1272, 2001.

Hashimoto, K., W. Calvert, and H. Matsumoto, Kilometric continuum detected by Geotail, *J. Geophys. Res.*, *104*, 28,645-28,656, 1999.

Horne, R. B., Path-integrated growth of electrostatic waves: The generation of terrestrial myriametric radiation, *J. Geophys. Res.*, *94*, 8895-8909, 1989.

Horne, R. B., Narrow-band structure and amplitude of terrestrial myriametric radiation, *J. Geophys. Res.*, *95*, 3925-3932, 1990.

Jones, D., Source of terrestrial non-thermal continuum radiation, *Nature*, *260*, 686, 1976.

Jones, D., Planetary radio emissions from low magnetic latitudes: Observations and theories, in *Planetary Radio Emissions II*, edited by H. O. Rucker, S. J. Bauer, and B. -M. Pedersen, pp. 255-293, Austrian Academy of Sciences, Graz, 1988.

Kurth, W. S., D. A. Gurnett, and R. R. Anderson, Escaping non-thermal continuum radiation, *J. Geophys. Res.*, *86*, 5519-5531, 1981.

Kurth, W. S., Detailed observations of the source of terrestrial narrowband electromagnetic radiation, *Geophys. Res. Lett.*, *9*, 1341-1344, 1982.

Kurth, W. S., Continuum radiation in planetary magnetospheres, in *Planetary Radio Emissions III*, ed. by H. O. Rucker, S. J. Bauer, and M. L. Kaiser, p. 329-350, Austrian Academy of Science, 1992.

Matsumoto, H., I. Nagano, R. R. Anderson, H. Kojima, K. Hashimoto, M. Tsutsui, T. Okada, I. Kimura, Y. Omura, and M. Okada, Plasma wave observations with GEOTAIL spacecraft, *J. Geomagn. Geoelectr.*, *46*, 59-95, 1994.

Melrose, D. B., A theory for the nonthermal radio continua in the terrestrial and Jovian magnetospheres, *J. Geophys. Res.*, *86*, 30-36, 1981.

Morgan, D. D., and D. A. Gurnett, The source location and beaming of terrestrial continuum radiation, *J. Geophys. Res.*, *86*, 9595-9613, 1991.

Moullard, O., A. Masson, J. Laasko, M. Parrot, P. Décréau, O.Santolik, and M. Andre, Density modulated whistler mode emissions observed near the plasmapause, *Geophys. Res. Lett.*, *29*, 1975, doi: 10.1029/2002GL015101, 2002.

Pedersen, A., N. Cornilleau Wehrlin, B. de la Porte, A. Roux, A. Bouabdellah, P. M. E. Decreau, F. Lefeuvre, F. X. Sene, D. Gurnett, R. Huff, G. Gustafsson, G. Holmgren, L.

Woolliscroft, H. S. Alleyne, J. A. Thompson, P. H. N. Davies, The wave experiment consortium (WEC), *Sp. Sci. Rev.*, *79* (1-2), 93-105, 1997.

Ronnmark, K., Emission of myriametric radiation by coalescence of upper hybrid waves with low frequency waves, *Ann. Geophys.*, 1, 187-192, 1983.

Ronnmark, K., Myriametric radiation and the efficiency of linear mode conversion, *Geophys. Res. Lett.*, *16*, 731-738, 1989.

Ronnmark, K. Conversion of upper hybrid waves into magnetospheric radiation, in *Planetary Radio Emissions III*, ed. by H. O. Rucker, S. J. Bauer, and M. L. Kaiser, p. 405-417, Austrian Academy of Science, 1992.

Figure Captions

Figure 1. In Figure 1 we display a frequency-time spectrogram of the Geotail plasma wave instrument (PWI) sweep-frequency analyzer (SFA) with relative power gray-coded. This spectrogram covers a six-hour period on May 20, 1996, when the spacecraft was on the nightside at a distance ranging from 15.75 R_E to 12.3 R_E, and ranging in magnetic latitude from 8.4° through the magnetic equator to -6.1°. The kilometric continuum emission is seen as the narrow-band frequency-drifting features indicated.

Figure 2. A frequency-time spectrogram of the PWI sweep-frequency receiver for a twenty-five minute period of day May 20, 1996. Here the MLT is near 22 hours and the spacecraft varies in radial distance from 4.11 to 3.58 R_E. The magnetic latitude varies in the polar orbit from 15° to < 4.7°. The top panel displays the electric field while the bottom panel shows the magnetic field data in a frequency range from 100 kHz to 250 kHz.

Figure 3. A much higher resolution PWI spectrogram of day May 20, 1996, that covers only two minutes of time. Here a spin modulation of the electric and magnetic field data is discernable. The spin period of the Polar satellite is about 6 seconds while the nulls in Figure 3 are about 10 seconds apart. This is due to an aliasing of the spin period with the instrument frequency cycling period of about 2.5 seconds.

Figure 4. In Figure 4 we show a spectrogram of Polar SFR data for a 55-minute period on day February 11, 1997. During this time period the spacecraft is located in the afternoon sector of MLT ranging from 15.0 hours to 16.1 hours. The radial distance varies from 2.11 R_E to 3.4 R_E.

Significantly the magnetic latitude varies from high southern latitudes, -38.2° through the magnetic equator to ~14.4°.

Figure 5. In Figure 5 we show Geotail observations for May 23, 1996. Polar observations for the period from 02:10 to 02:32 are compared in Figure 6. We note that Geotail at this time is located at R ~30.25 R_E, MLT ~14.55 hours, and λ_m ~14.1 degrees, while Polar was in the range 3.1 R_E < R < 3.7 R_E, -4.9° < λ_m < 7.75°, and 21.9 hours < MLT < 22 hours. Thus, the MLT of Polar is about 8 hours different from that of Geotail.

Figure 6. Electric and magnetic field data observed by Polar for a portion of the time period shown in Figure 5 (Geotail). We observe several bands of UH emission in the electric antenna and a few bands of EM emission in the magnetic field data of the lower panel. Spin modulation is clearly seen in the Polar data which allows us to speculate on the wave modes present.

Figure 7. We show an example of Polar SFR data for May 15, 1996. The spacecraft is located in the range 3.8 < R < 5.3 R_E, -7.0° < λ_m < 13.2 °, and MLT ~22.3 hours. The interesting aspect of this data is the clear oscillation of the UH signature in both the electric and magnetic field indicating a probable density fluctuation, perhaps due to the spacecraft crossing a density duct or encountering a density cavity. In the magnetic field data (lower panel) there are interference lines located at f = 50 kHz, and f = 100 kHz.

Figure 8. Polar SFR spectrogram for a magnetic equator crossing on April 10, 1996. This data looks typical of many of the other crossings of the magnetic equator, this time located at MLT

~0.35 and r ~4.5 R_E. There is some rather intense electric field emission and faint, but distinct magnetic oscillations observed in the interval from about 15:27 to 15:32. For this crossing, however, high resolution data shown in Figure 9 is also available.

Figure 9. Spectrogram of the high resolution wideband receiver data for a 48-second time interval starting at 15:30.046. This data covers a frequency range from 125 kHz to about 215 kHz, which includes the EM emission seen in Figure 8. Of particular significance are the many relatively intense near-constant frequency emission bands. The frequency separation of these bands is much less than the local electron cyclotron frequency. There is also a spin-modulation of the data showing nulls at ~3 second intervals. This modulation is consistent with electrostatic UH emission for the most intense bands in the interval 150 kHz < f < 170 kHz. For f > 170 kHz the emission nulls are ~90° out of phase with those for f < 170 kHz, and are consistent with ordinary mode emission.

Figure 10. A spectrogram of the wideband instrument (WBD) on board the Cluster (SC2) spacecraft. The spectrogram covers a frequency range from 250 kHz to 260 kHz over a 30-second time interval. SC2 is located just above the magnetic equator at λ_m ~3.2°, R = 4.36 R_E and MLT ~17 hours. Seen in the figure are very many closely-spaced emission bands that increase slightly in frequency over the 30 second period of the plot. Spin modulation lanes are also seen at about 2 second intervals. The similarity between this plot and Figure 9 is striking.

GEOTAIL PWI SFA

96–141 (MAY 20) 02:00:00 UT 06 hrs

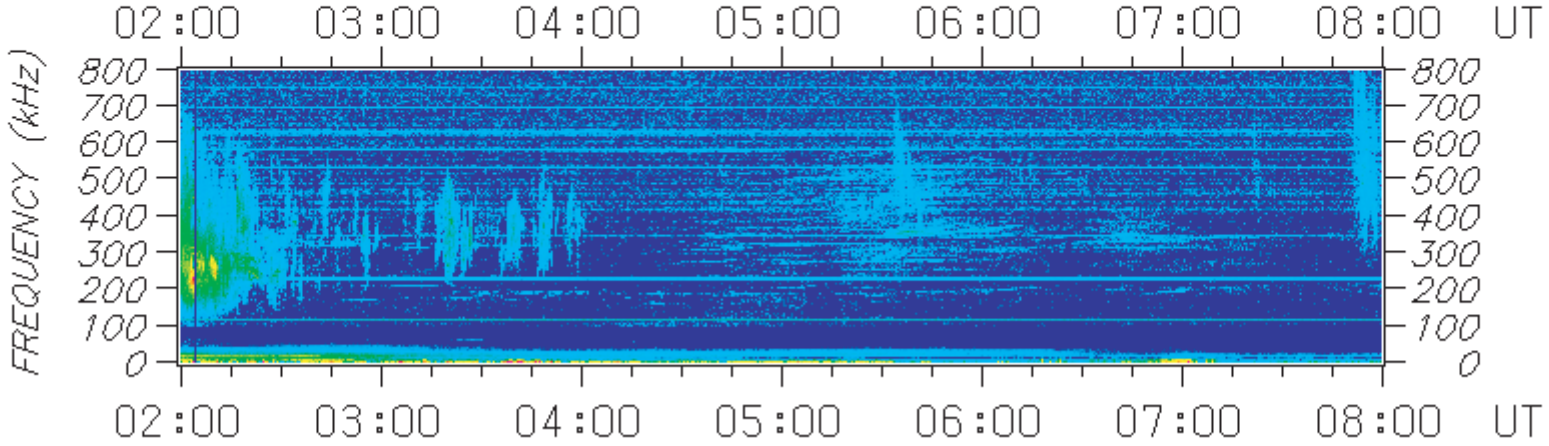

XGSE	=	-9.93 RE	-10.37 RE	-10.75 RE	-11.07 RE	-11.31 RE	-11.45 RE	-11.49 RE
YGSE	=	12.22 RE	11.06 RE	9.83 RE	8.54 RE	7.19 RE	5.78 RE	4.32 RE
ZGSE	=	0.36 RE	0.48 RE	0.59 RE	0.70 RE	0.80 RE	0.90 RE	0.99 RE
R	=	15.75 RE	15.17 RE	14.58 RE	14.00 RE	13.42 RE	12.86 RE	12.32 RE
YGSM	=	11.40 RE	10.43 RE	9.38 RE	8.23 RE	6.98 RE	5.65 RE	4.24 RE
ZGSM	=	4.43 RE	3.71 RE	3.02 RE	2.40 RE	1.90 RE	1.53 RE	1.29 RE
GMLAT	=	8.39°	6.74°	4.68°	2.28°	-0.39°	-3.22°	-6.14°
GMLONG	=	351.72°	340.63°	329.99°	319.86°	310.26°	301.23°	292.80°
MLT	=	20.87 HRS	21.08 HRS	21.32 HRS	21.60 HRS	21.91 HRS	22.26 HRS	22.65 HRS
" HR:MN	=	20:52	21:05	21:19	21:36	21:55	22:16	22:39

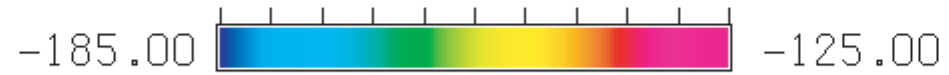

EDITOR B RRAVAX$DKA500:[DATA.GE.SDJ96052001.S01;1

GTLSFA5L V1.6 PROCESSED 18-JUN-02 16:38

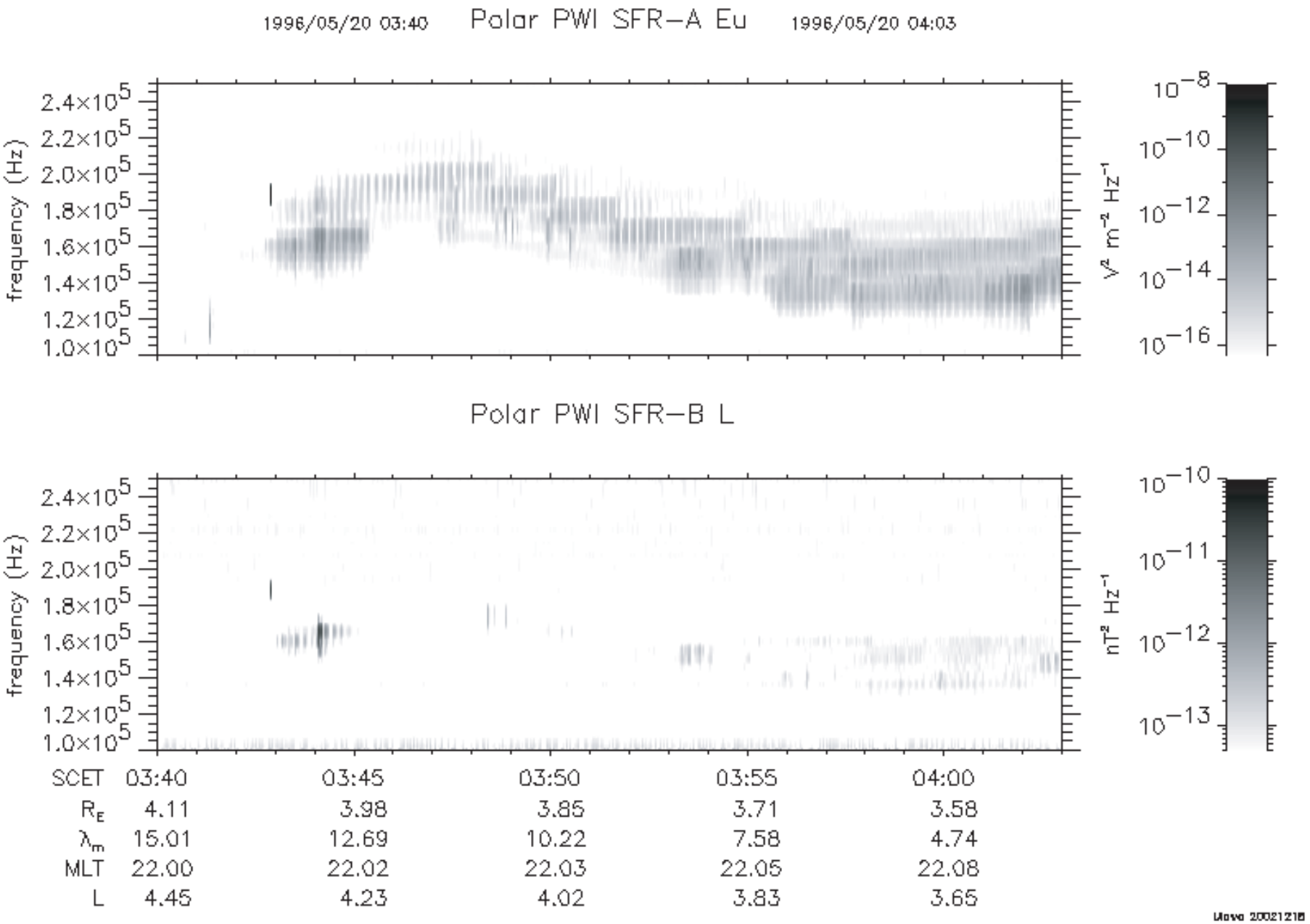
1996/05/20 03:40
Polar PWI SFR-A Eu
1996/05/20 04:03
frequency (Hz)
2.4×10^5
2.2×10^5
2.0×10^5
1.8×10^5
1.6×10^5
1.4×10^5
1.2×10^5
1.0×10^5
V² m⁻² Hz⁻¹
10^-8
10^-10
10^-12
10^-14
10^-16
Polar PWI SFR-B L
nT² Hz⁻¹
10^-10
10^-11
10^-12
10^-13
SCET 03:40 03:45 03:50 03:55 04:00
R_E 4.11 3.98 3.85 3.71 3.58
λ_m 15.01 12.69 10.22 7.58 4.74
MLT 22.00 22.02 22.03 22.05 22.08
L 4.45 4.23 4.02 3.83 3.65
Wave 20021218

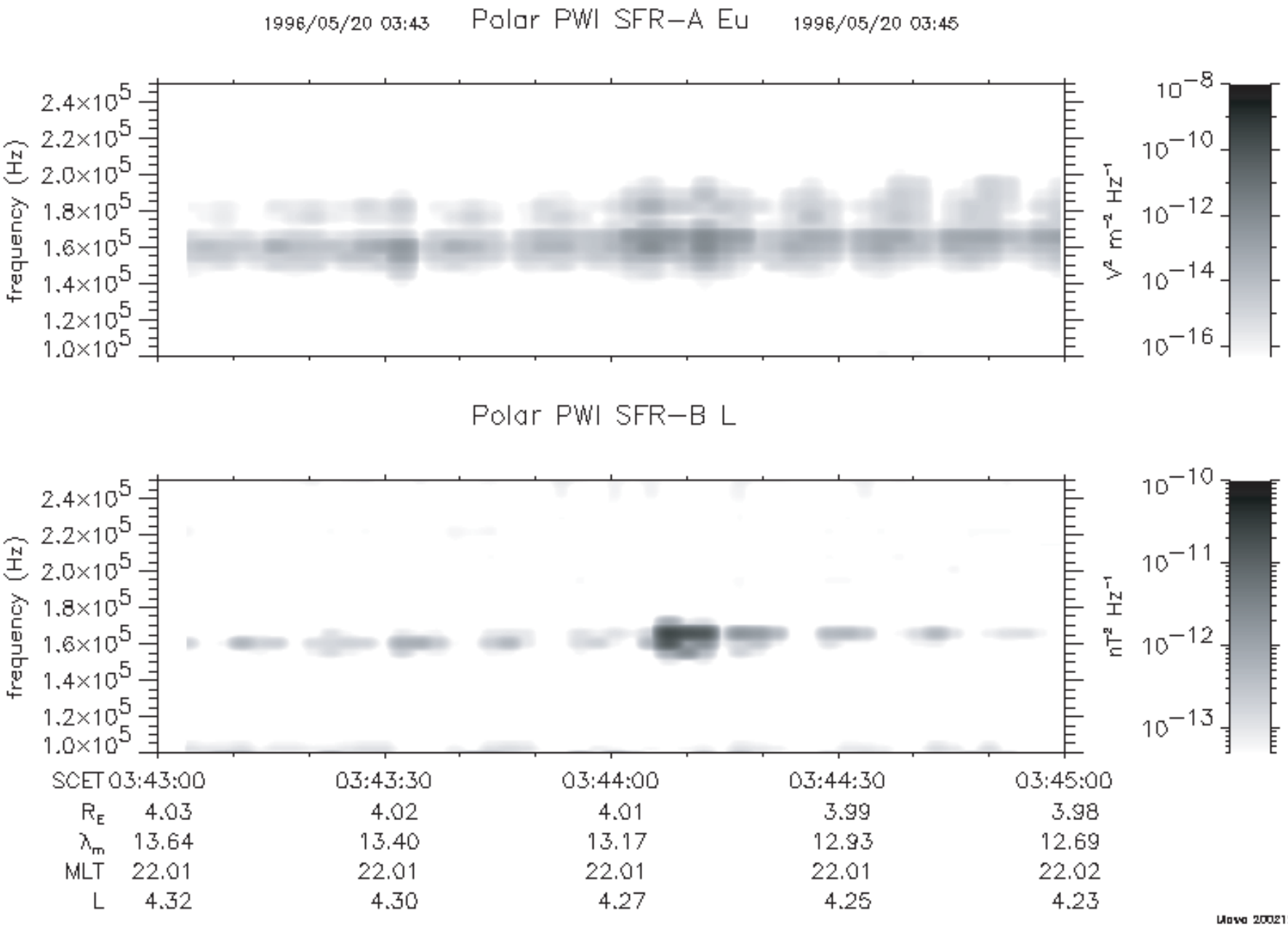
1996/05/20 03:43
Polar PWI SFR-A Eu
1996/05/20 03:45
frequency (Hz)
2.4×10^5
2.2×10^5
2.0×10^5
1.8×10^5
1.6×10^5
1.4×10^5
1.2×10^5
1.0×10^5
V² m⁻² Hz⁻¹
10^-8
10^-10
10^-12
10^-14
10^-16
Polar PWI SFR-B L
frequency (Hz)
nT² Hz⁻¹
10^-10
10^-11
10^-12
10^-13
SCET 03:43:00 03:43:30 03:44:00 03:44:30 03:45:00
R_E 4.03 4.02 4.01 3.99 3.98
λ_m 13.64 13.40 13.17 12.93 12.69
MLT 22.01 22.01 22.01 22.01 22.02
L 4.32 4.30 4.27 4.25 4.23
Wave 20021218

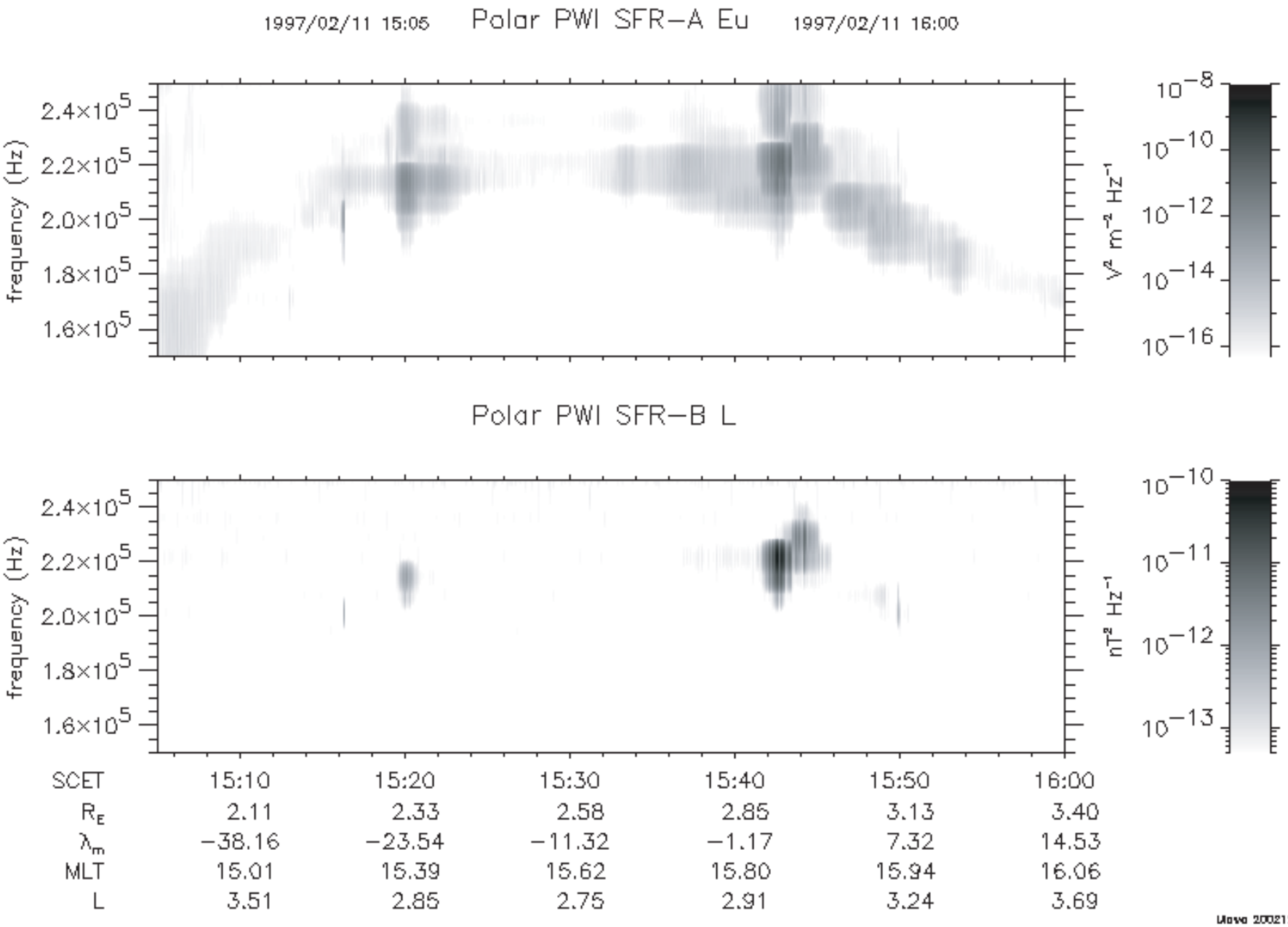
1997/02/11 15:05
Polar PWI SFR−A Eu
1997/02/11 16:00
frequency (Hz)
2.4×10^5
2.2×10^5
2.0×10^5
1.8×10^5
1.6×10^5
V² m⁻² Hz⁻¹
10^−8
10^−10
10^−12
10^−14
10^−16
Polar PWI SFR−B L
frequency (Hz)
2.4×10^5
2.2×10^5
2.0×10^5
1.8×10^5
1.6×10^5
nT² Hz⁻¹
10^−10
10^−11
10^−12
10^−13
SCET 15:10 15:20 15:30 15:40 15:50 16:00
R_E 2.11 2.33 2.58 2.85 3.13 3.40
λ_m −38.16 −23.54 −11.32 −1.17 7.32 14.53
MLT 15.01 15.39 15.62 15.80 15.94 16.06
L 3.51 2.85 2.75 2.91 3.24 3.69
Wave 20021218

GEOTAIL PWI SFA

96-144 (MAY 23) 00:00:00 UT 10 hrs

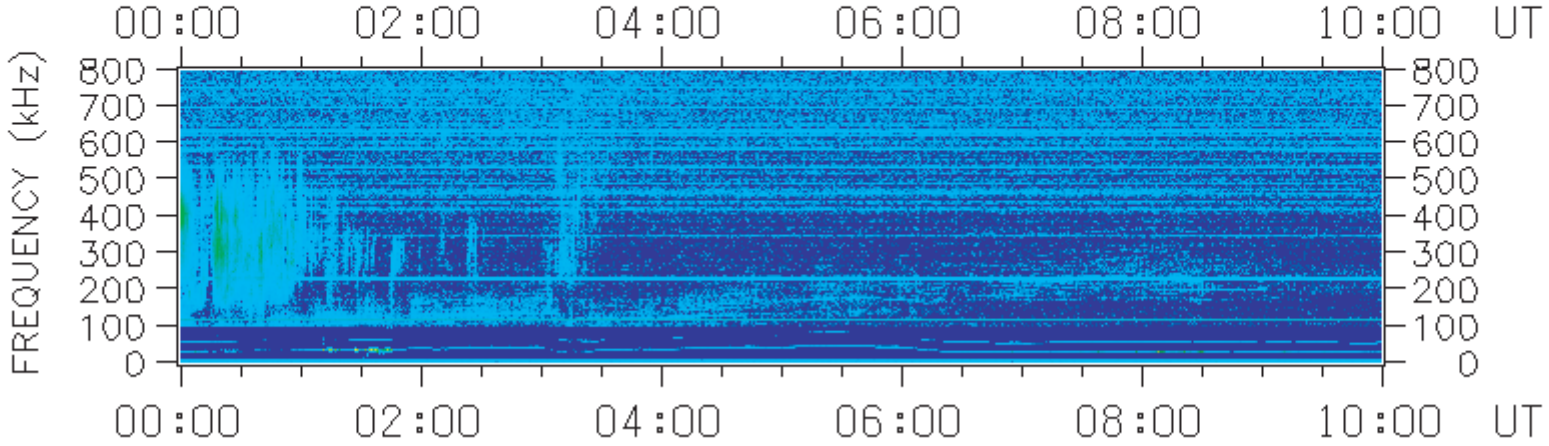

XGSE =	24.69 RE	24.17 RE	23.58 RE	22.92 RE	22.21 RE	21.43 RE
YGSE =	16.88 RE	17.86 RE	18.79 RE	19.68 RE	20.51 RE	21.28 RE
ZGSE =	-3.58 RE	-3.57 RE	-3.55 RE	-3.53 RE	-3.49 RE	-3.44 RE
R =	30.12 RE	30.26 RE	30.36 RE	30.42 RE	30.43 RE	30.40 RE
YGSM =	16.99 RE	18.07 RE	19.11 RE	19.97 RE	20.66 RE	21.30 RE
ZGSM =	2.99 RE	2.28 RE	0.89 RE	-0.82 RE	-2.39 RE	-3.34 RE
GMLAT =	19.36°	14.19°	9.54°	6.39°	5.39°	6.74°
GMLONG =	284.08°	256.73°	229.86°	203.06°	176.19°	149.31°
MLT =	14.45 HRS	14.53 HRS	14.64 HRS	14.76 HRS	14.87 HRS	14.99 HRS
" HR:MN =	14:27	14:32	14:39	14:45	14:52	14:59

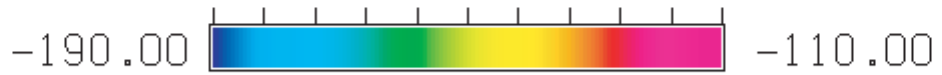

EDITOR B RRAVAX$DKA500:[DATA.GE.SDJ96052301.S01;1

GTLSFA5L V1.6 PROCESSED 19-JUN-02 10:36

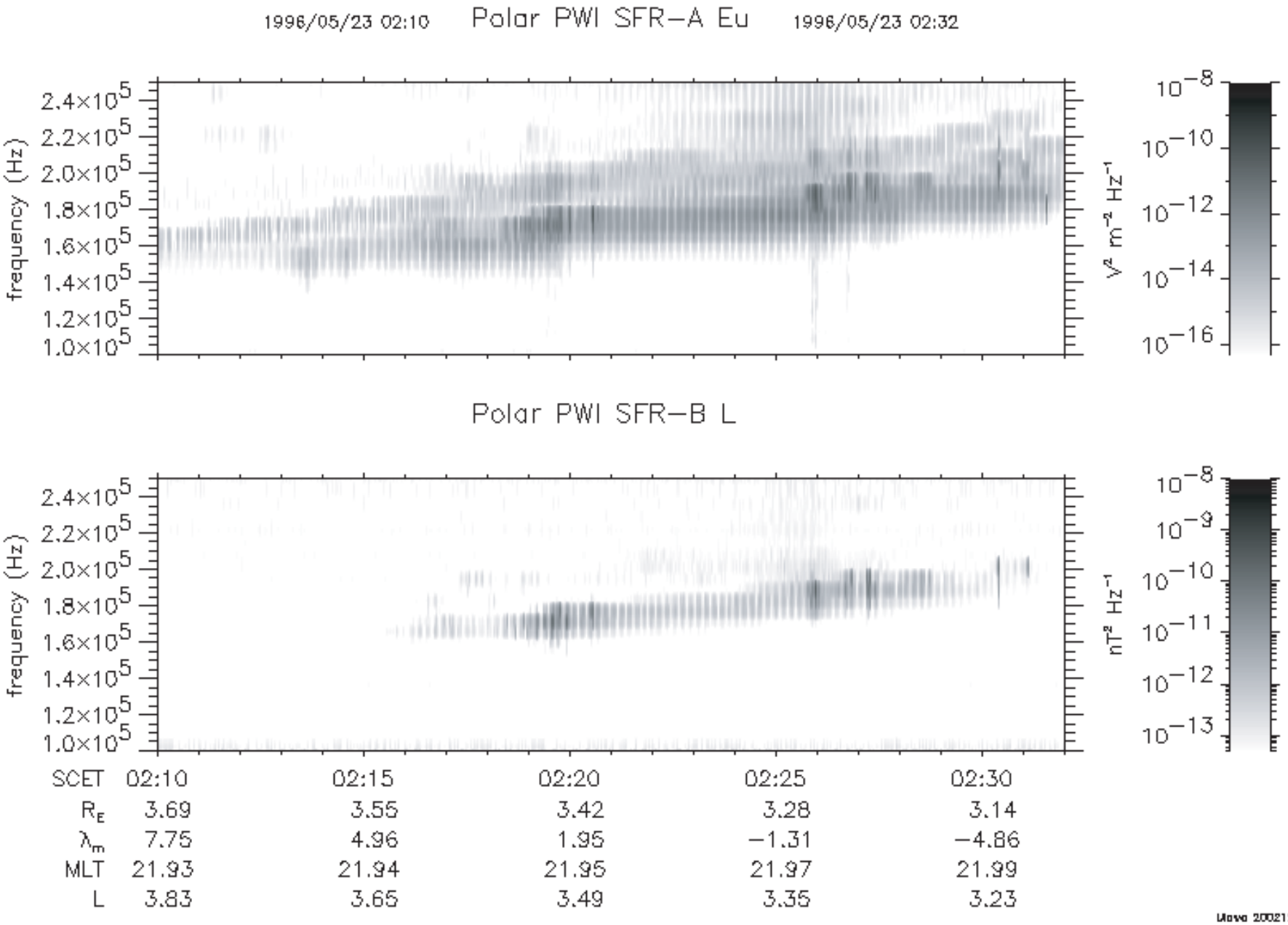
1996/05/23 02:10
Polar PWI SFR-A Eu
1996/05/23 02:32
frequency (Hz)
2.4×10^5
2.2×10^5
2.0×10^5
1.8×10^5
1.6×10^5
1.4×10^5
1.2×10^5
1.0×10^5
V² m⁻² Hz⁻¹
10^-8
10^-10
10^-12
10^-14
10^-16
Polar PWI SFR-B L
nT² Hz⁻¹
10^-8
10^-9
10^-10
10^-11
10^-12
10^-13
SCET 02:10 02:15 02:20 02:25 02:30
R_E 3.69 3.55 3.42 3.28 3.14
λ_m 7.75 4.96 1.95 −1.31 −4.86
MLT 21.93 21.94 21.95 21.97 21.99
L 3.83 3.65 3.49 3.35 3.23
Wave 20021218

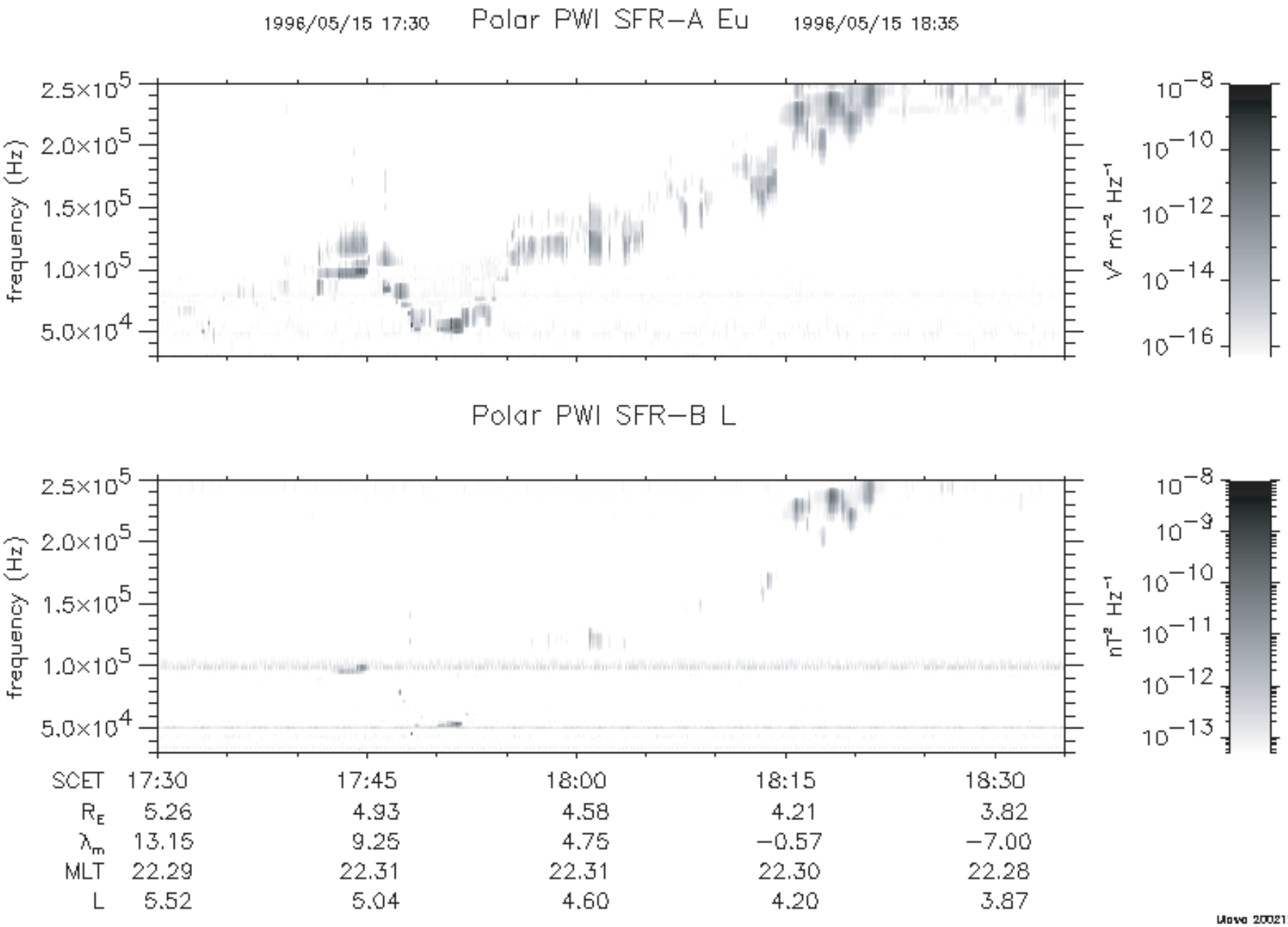
1996/05/15 17:30
Polar PWI SFR-A Eu
1996/05/15 18:35
frequency (Hz)
2.5×10^5
2.0×10^5
1.5×10^5
1.0×10^5
5.0×10^4
V² m⁻² Hz⁻¹
10^-8
10^-10
10^-12
10^-14
10^-16
Polar PWI SFR-B L
frequency (Hz)
2.5×10^5
2.0×10^5
1.5×10^5
1.0×10^5
5.0×10^4
nT² Hz⁻¹
10^-8
10^-9
10^-10
10^-11
10^-12
10^-13
SCET 17:30 17:45 18:00 18:15 18:30
R_E 5.26 4.93 4.58 4.21 3.82
λ_m 13.15 9.25 4.75 −0.57 −7.00
MLT 22.29 22.31 22.31 22.30 22.28
L 5.52 5.04 4.60 4.20 3.87
Wave 20021218

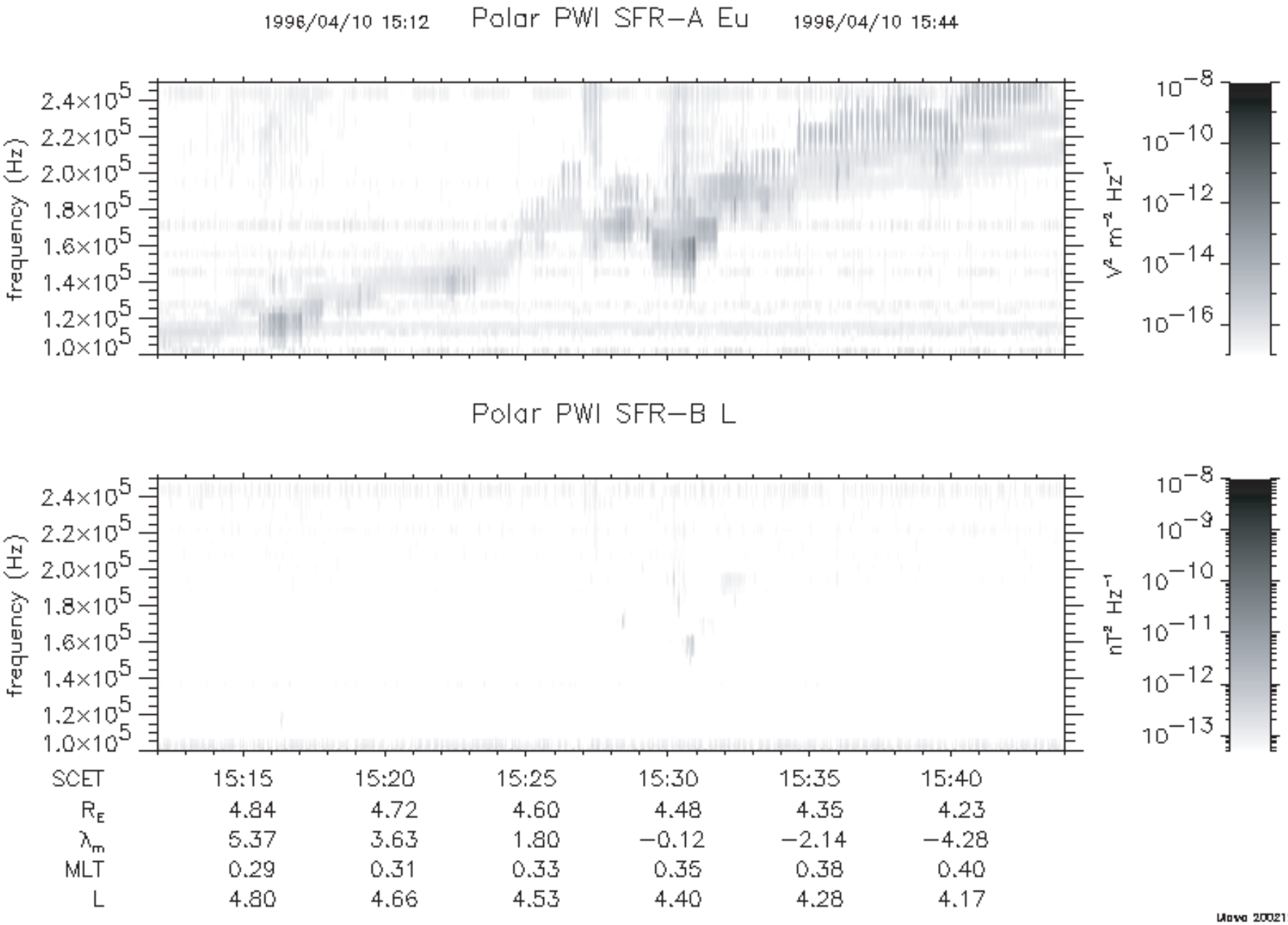
1996/04/10 15:12
Polar PWI SFR−A Eu
1996/04/10 15:44
frequency (Hz)
2.4×10^5
2.2×10^5
2.0×10^5
1.8×10^5
1.6×10^5
1.4×10^5
1.2×10^5
1.0×10^5
V² m⁻² Hz⁻¹
10^−8
10^−10
10^−12
10^−14
10^−16
Polar PWI SFR−B L
frequency (Hz)
nT² Hz⁻¹
10^−8
10^−9
10^−10
10^−11
10^−12
10^−13
SCET 15:15 15:20 15:25 15:30 15:35 15:40
R_E 4.84 4.72 4.60 4.48 4.35 4.23
λ_m 5.37 3.63 1.80 −0.12 −2.14 −4.28
MLT 0.29 0.31 0.33 0.35 0.38 0.40
L 4.80 4.66 4.53 4.40 4.28 4.17
Wave 20021218

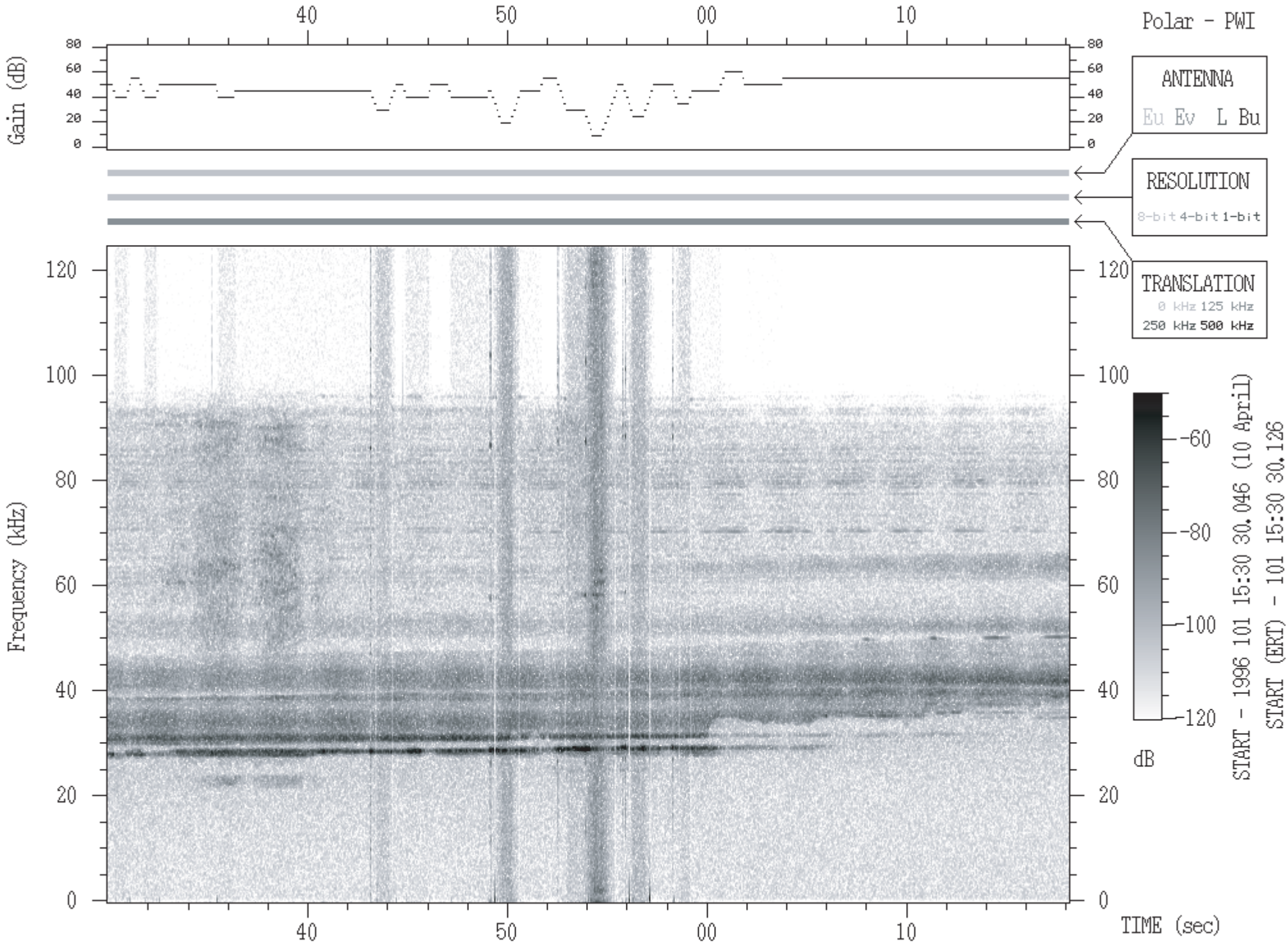
Polar - PWI
40
50
00
10
Gain (dB)
80
60
40
20
0
ANTENNA
Eu Ev L Bu
RESOLUTION
8-bit 4-bit 1-bit
TRANSLATION
0 kHz 125 kHz
250 kHz 500 kHz
Frequency (kHz)
120
100
80
60
40
20
0
-60
-80
-100
-120
dB
START - 1996 101 15:30 30.046 (10 April)
START (ERT) - 101 15:30 30.126
TIME (sec)

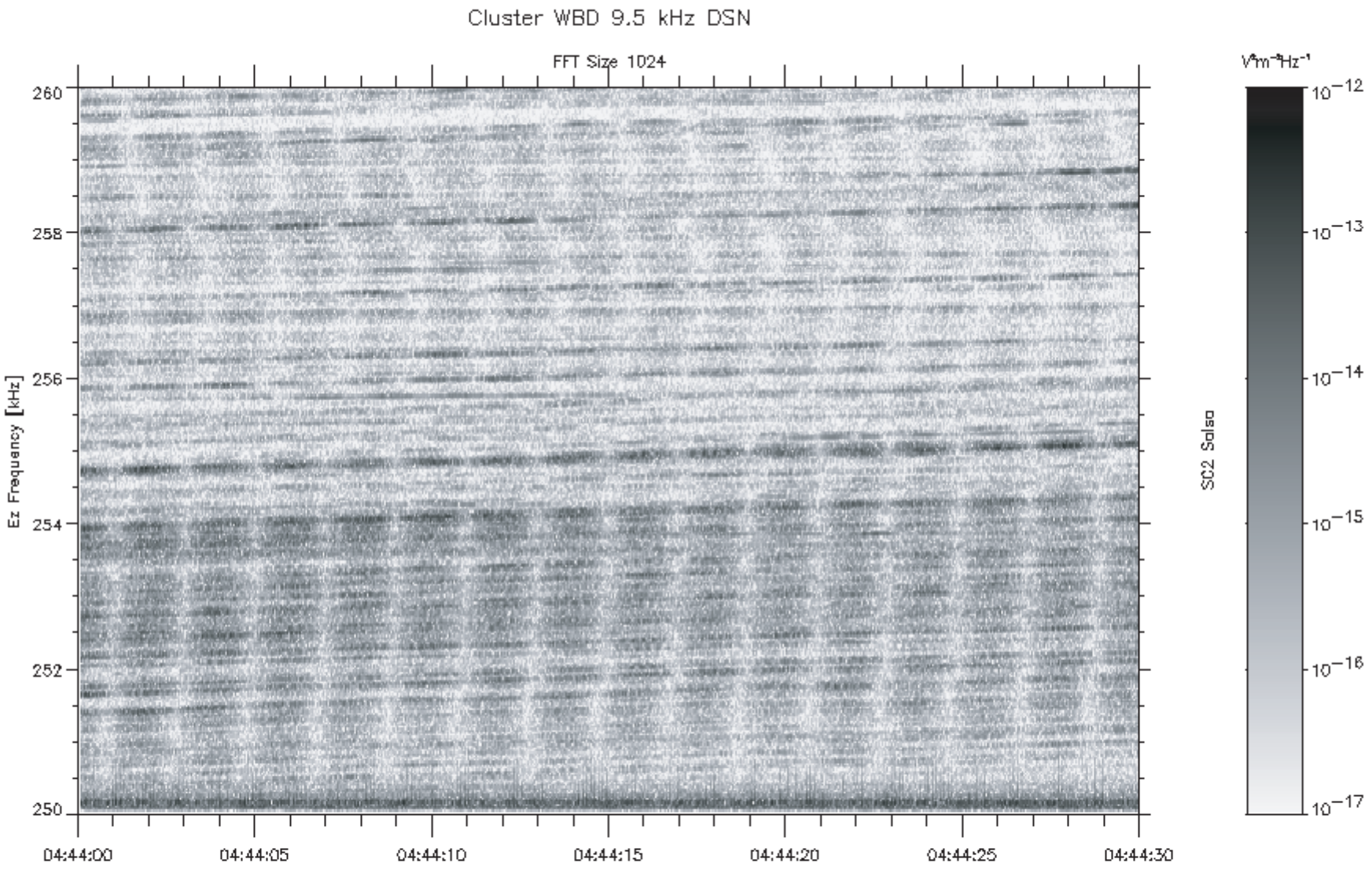

R_E	4.36	4.36	4.36	4.36	4.36	4.36	4.36
λ_m	3.05	3.10	3.14	3.19	3.23	3.28	3.32
MLT	16.99	16.99	16.99	16.98	16.98	16.98	16.98
L	4.40	4.40	4.40	4.40	4.40	4.40	4.40

UT_OBT: 2002-06-19T04:44:00 to 2002-06-19T04:44:30

Ulowa 021227